Effect of neutralizing cation type on the morphology and properties of model polyurethane ionomers

Susan A. Visser and Stuart L. Cooper*
Department of Chemical Engineering, University of Wisconsin–Madison, Madison, WI 53706, USA
(Received 26 September 1990; revised 16 January 1991; accepted 22 January 1991)

The influence of cation type on the morphology and properties of model polyurethane ionomers is investigated in ionomers with different backbone types, pendant anion types and ionic group concentrations. A correlation between the degree of ordering in the local environment of the neutralizing cation and the tensile properties of the ionomers is observed. The geometrical packing constraints of the pendant anion are also seen to be a critical factor in determining the physical properties of ionomers. Differential scanning calorimetry results indicate no significant differences in the extent of phase separation of ionomers neutralized with different cations; however, anion type is shown to have a large influence on the degree of phase separation. Small-angle X-ray scattering analysis of the morphology of the ionomers reveals a correlation between the number of ionic groups per aggregate and the low-temperature storage modulus measured by dynamic mechanical analysis. The importance of the electronic structure and geometrical packing constraints of the ionic groups is emphasized.

(Keywords: ionomer; polyurethane ionomer; structure–property relationships; small-angle X-ray scattering; neutralizing cation)

INTRODUCTION

Macromolecules containing a small number of ionic groups covalently bound to a non-polar chain are known as ionomers. In the bulk, the large polarity difference between the ionic groups and the polymer chain causes microphase separation, resulting in the formation of ionic aggregates in the polymer matrix. The ionic aggregates act as physical crosslinks in the system, imparting dramatic changes in material properties[1–6]. Exploitation of the enhanced properties of ionomers has led to a wide variety of unique applications[7,8], as well as the recognition that an increased understanding of these systems is necessary to exploit fully their unusual properties.

A number of factors have been shown to influence ionomer properties, including the placement of ionic groups[9], the concentration of ionic groups[10], the length of the spacer between the ionic groups and the polymer chain[11,12], the compatibility of the polymer chain and the ionic groups[13], the nature of the pendant anion[14–16], and the choice of neutralizing cation[13,17–19]. The effect of neutralizing cation type has been studied extensively in random copolymer ionomers[4,6,20]. However, in a recent small-angle X-ray scattering (SAXS) study of narrow and broad molecular-weight distribution sulphonated polystyrene (SPS) ionomers, the presence of fine structure on the ionomer peak of the sodium-neutralized ionomer was observed only in the polymer with the narrow molecular-weight distribution[21]. Thus, some of the information regarding structure–property relationships in ionomers may have been hidden in previous studies because broad molecular-weight distribution random copolymer ionomers were examined. Studies of telechelic ionomers do not have this drawback and have provided a wealth of information on the role of the neutralizing cation in ionomer structure–property relationships[4,6,17,18]. However, it has recently been argued[22] that the vastly differing architectures of telechelic and random copolymer ionomers make telechelic ionomers questionable models for random copolymer ionomers.

In order to address more carefully the role of the neutralizing cation, it would be desirable to study the effect of neutralizing cation type in a system that combines the regular chain architecture of the telechelics with a distribution of ionic groups along the polymer chain, as is found in the random copolymer ionomers. Towards this goal, a study was undertaken to probe the morphology and properties of a series of model polyurethane ionomers neutralized with sodium (Na^+) or one of four divalent cations (Cd^{2+}, Ni^{2+}, Sr^{2+} or Ca^{2+}). The polyurethane ionomers are excellent model systems because the ionic groups appear only at the urethane linkages and the polyols that separate the ionic groups have low polydispersities (< 1.5). Different polyol types, ion contents and pendant anion types were examined to determine the interplay between cation type and other ionomer structural variables.

EXPERIMENTAL

Sample preparation

The synthesis of the model polyurethane ionomers was described in the previous paper[14]. The model poly-

* To whom correspondence should be addressed
0032-3861/92/050920-10

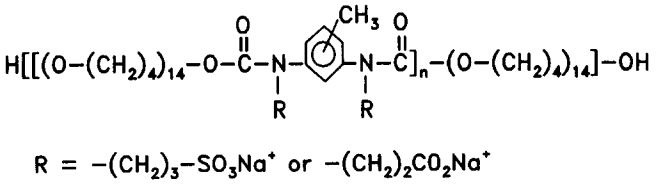

Figure 1 Structure of the model polyurethane ionomer, sodium form, using PTMO(1000) polyol as an example. n is the overall degree of polymerization

urethane ionomers are 1:1 copolymers of a polyol and toluene diisocyanate (TDI), which have propyl sulphonate or ethyl carboxylate groups grafted solely at the urethane linkages. The base polyurethanes had molecular weights in excess of 50000 in all cases. A typical model polyurethane ionomer chemical structure is shown in *Figure 1*. Two polyol types were investigated: poly(tetramethylene oxide) (PTMO, M_n = 990, 2070) and poly(propylene oxide) (PPO, average molecular weight 1000, 2000). The sodium-neutralized ionomers were obtained directly from the grafting reaction. Ionomers neutralized with other cations were obtained by ion-exchange procedures, as described previously[13]. Nickel, calcium or cadmium acetate, or strontium isopropoxide were used as neutralizing agents.

All ionomers were examined as solution-cast films. The sulphonated ionomers were cast at 60°C from *N,N*-dimethylacetamide. The carboxylated ionomers were cast at 25°C from 4:1 v/v toluene/methanol, except for the 98% carboxylated PTMO(1000)/TDI ionomers because of solubility constraints. (The parenthetical '1000' indicates the approximate molecular weight of the PTMO polyol.) The 98% carboxylated PTMO(1000)/TDI ionomers were cast from 2:1 v/v toluene/methanol solutions. Films were dried in a 50°C vacuum oven for at least one week before testing to remove residual solvent and water. It should be noted that complete removal of all residual water or polar solvents from ionomers is extremely difficult, as polar solvents tend to complex strongly with the ionic groups. Thus, while this drying procedure is the most stringent possible without causing significant polymer degradation, it may still be insufficient to give completely 'dry' ionomers. Residual water may cause some changes in ionomer properties, but the comparisons made in this paper are still expected to be valid for the typical use conditions of ionomers.

Instrumental conditions

Samples for uniaxial stress–strain testing were stamped out with a standard ASTM D1708 die and were tested using an Instron TM model at room temperature in air, with a crosshead speed of 0.5 inch min^{-1} (12.7 mm min^{-1}). Differential scanning calorimetry (d.s.c.) thermograms were recorded using a Perkin–Elmer DSC-7. Sample weights were 11 ± 2 mg. Thermograms were recorded from -130 to 150°C at a heating rate of 20°C min^{-1}. Dynamic mechanical thermal analysis (d.m.t.a.) data were obtained using a Rheometrics RSA-II at a test frequency of 100 rad s^{-1} (15.9 Hz) under a dry nitrogen purge. Temperature steps of 3°C/step were used, with 0.1 min equilibration time at each step.

SAXS measurements

The small-angle X-ray scattering (SAXS) data were obtained using an Elliot GX-21 rotating-anode generator, an Anton-Paar compact Kratky scattering camera and a TEC model 211 linear position-sensitive detector. Cu Kα radiation was monochromatized using a nickel filter and pulse-height discrimination. The scattering camera has a sample-to-detector distance of 60 cm and a detector length of approximately 8 cm. This configuration allowed a q ($q = (4\pi/\lambda)\sin\theta$, where 2θ is the scattering angle and λ is the wavelength of the radiation) range of 5.7 nm^{-1}, with a minimum q of 0.15 nm^{-1} due to the position of the beam stop, to be probed. The detector length was divided into 128 channels for a resolution of $\simeq 0.05$ nm^{-1}. All data were collected at room temperature.

The data were corrected for detector sensitivity, parasitic and background scattering, and absorption of X-rays by the sample. The beam profile along the slit length was measured and the iterative method developed by Lake[23] was used to desmear the data. Absolute intensities expressed in terms of I/I_eV, where I_e is the intensity scattered by a single electron and V is the scattering volume, were determined by comparing the sample scattering intensity to that from a calibrated Lupolen (polyethylene) standard[24]. Background scattering was determined by fitting the SAXS data in the high-q region using Porod's law[25] plus a constant background term.

Sample nomenclature

Samples are designated with the first letter indicating the soft-segment type (M = PTMO, P = PPO), the number indicating the soft-segment molecular weight in thousands, the letter describing pendant ionic-group type (S = sulphonate, C = carboxylate) and the final two letters giving the chemical symbol for the neutralizing cation. Thus, M1SNa indicates the 1:1 copolymer of PTMO, molecular weight 1000, and TDI, sulphonated and neutralized with sodium. Polymer backbone types may also be indicated in the text by the three- or four-letter abbreviation for the soft-segment type, followed by the soft-segment molecular weight in parentheses. For example, ionomers based on a 1:1 copolymer of PTMO, molecular weight 1000, and TDI may be described as PTMO(1000)-based ionomers.

RESULTS AND DISCUSSION

Tensile testing

The uniaxial stress–strain curves for the model polyurethane ionomers are shown in *Figures 2–4*. The Young's modulus and the stress (σ_b) and strain (ε_b) at break for each material are listed in *Table 1*. As can be seen in *Figures 2–4*, as the polyol molecular weight increases, Young's modulus decreases, as expected based on differing ion contents and resultant molecular weights between crosslinks. Examination of *Figures 2–4* also clearly shows that both neutralizing cation and pendant anion type strongly influence the large-deformation properties of the polyurethane ionomers. As had been seen in a previous study of lower-molecular-weight sulphonated PTMO(1000)/TDI ionomers[7], the Ni^{2+}-neutralized ionomer displays the most brittle tensile characteristics, followed by the Na^+-neutralized ionomer, with M1SCd displaying the most rubbery characteristics. Previous studies[7,26] suggested a direct correlation between the degree of order in the local environment around the neutralizing cation and the tensile properties of these

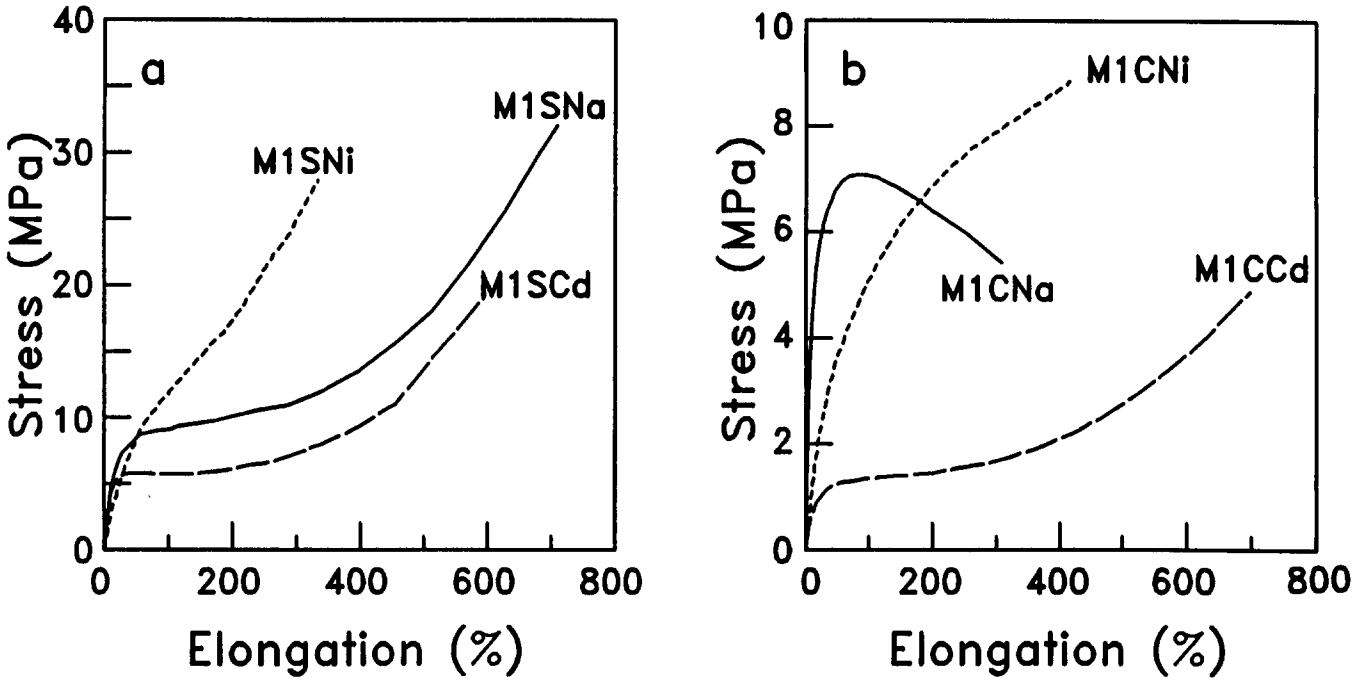

Figure 2 Uniaxial stress–strain results for (a) sulphonated PTMO(1000)-based ionomers and (b) carboxylated PTMO(1000)-based ionomers neutralized with various cations

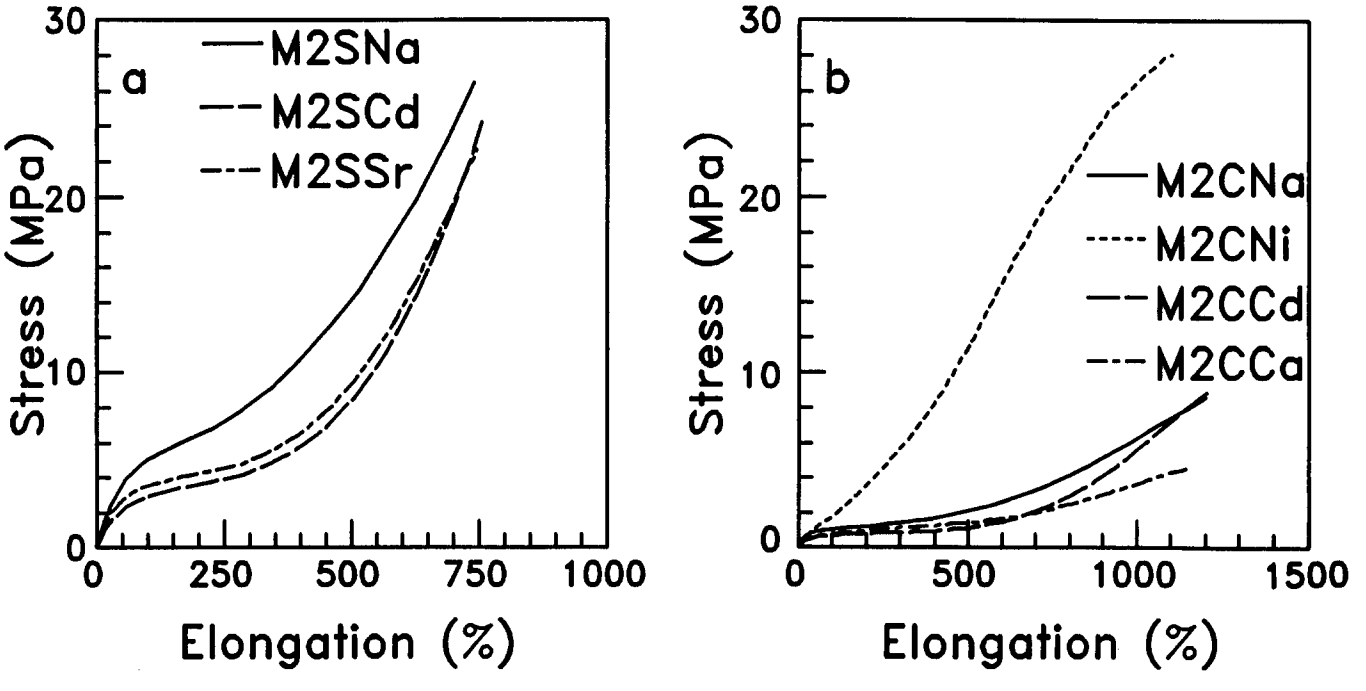

Figure 3 Uniaxial stress–strain results for (a) sulphonated PTMO(2000)-based ionomers and (b) carboxylated PTMO(2000)-based ionomers neutralized with various cations

ionomers. Assuming that increased polymer overall molecular weight does not change the local packing arrangements in the ionic aggregates, a correlation between tensile properties and local order is again observed. The rubbery characteristics of the sulphonated ionomers increase in the order M1SNi to M1SNa to M1SCd, while the degree of local ordering decreases from M1SNi to M1SCd[26].

A correlation between local ordering and tensile properties is also observed in the other model polyurethane ionomers. The decrease of the Young's modulus of the M1C ionomers in the order $Na^+ > Ni^{2+} > Cd^{2+}$ is matched by a similar decrease in local order. Extended X-ray absorption fine structure spectroscopy (e.x.a.f.s.) analysis of the local environments of the neutralizing cation in M1CNi and M1CCd showed local order decreasing from the two or more distinct coordination shells in the Ni^{2+} ionomer to the single disordered coordination shell in the Cd^{2+} ionomer[27]. Suggestions of an ordered local structure in M1CNa appear in the dynamic mechanical thermal analysis (d.m.t.a.) data, shown below, where a high-temperature ionic transition[14] is seen at ~100°C for the Na^+ ionomer, but not the Ni^{2+} or Cd^{2+} ionomers, suggesting a more highly

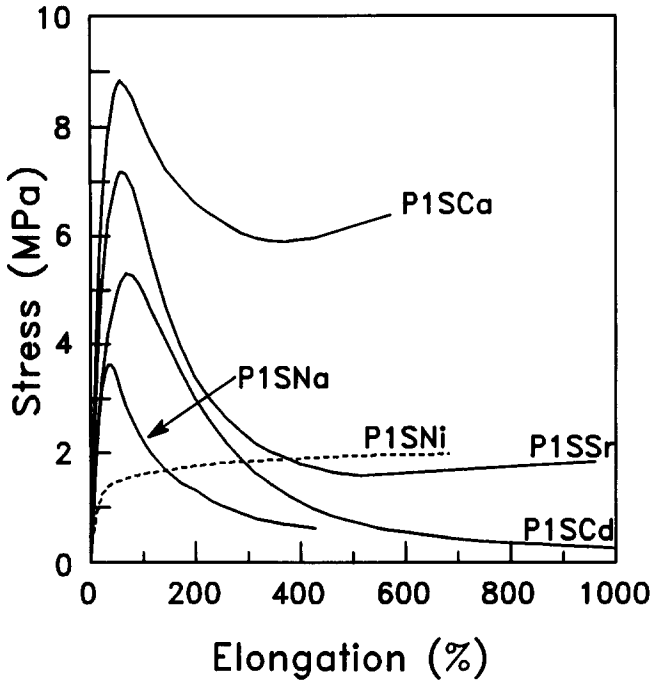

Figure 4 Uniaxial stress–strain results for sulphonated PPO(1000)-based ionomers neutralized with various cations

ordered local structure for M1CNa. For the M2S ionomers, the Young's moduli decrease in the order $Na^+ > Sr^{2+} > Cd^{2+}$. The d.m.t.a. results for M2SNa, shown below, exhibit some higher-temperature ionic transitions in the storage modulus *versus* temperature curve, which could indicate a high degree of local ordering. Furthermore, the e.x.a.f.s. results presented in the accompanying paper indicate a locally ordered structure in M2SSr and a disordered cation environment in M2SCd[27]. Thus, a match between local order and tensile properties is also observed in the M2S ionomers.

The correlation further holds for the M2C ionomers, where the Young's moduli decrease in the order $Na^+ > Ni^{2+} > Cd^{2+} > Ca^{2+}$, and e.x.a.f.s. analysis[27] of M2CNi and M2CCd indicates a matching decrease in local order. D.m.t.a. results for M2CNa, shown below, again display a high-temperature ionic transition, which suggests a high extent of local ordering.

Finally, the σ_b values for the P1S ionomers decrease in the order $Ca^{2+} > Ni^{2+} > Sr^{2+} > Na^+$, with P1SCd displaying no break point due to viscous flow. E.x.a.f.s. results[27] indicate the presence of at least two distinct coordination shells for the Ni^{2+} cation, one for Sr^{2+} and a disordered local environment for Cd^{2+}. The more highly ordered local environments allow greater stress levels to be achieved before failure of the sample.

Local ordering arguments also rationalize the differences seen between sulphonated and carboxylated ionomers. Comparison of *Figures 2a* and *2b* shows different trends in tensile properties for the sulphonated and carboxylated ionomers as neutralizing cation type is varied. The geometry of the ionic components could give rise to these differences. The carboxylate anion is planar with only one edge available for bonding to a cation[28]. In contrast, the sulphonate anion is tetrahedral[28] and has two possible coordination lengths for the cation, one (0.82 Å) if the cation coordinates to the edge of the anion and another (0.47 Å) if the cation coordinates to the face[29]. Thus, packing arrangements of the anions and cations would be expected to be very different in the sulphonated and carboxylated ionomers, leading to different results when the neutralizing cation type is varied.

Consideration of local ion distribution in the ionic aggregates also rationalizes the higher Young's moduli of M1CNa compared to M1CNi and M1CCd. As Lefelar and Weiss discussed[29], if packing arrangements consistent with the crystalline structures of low-molecular-weight ionic compounds are postulated for the monovalent and divalent cations of carboxylated ionomers, more anions will have to be shared by cations when the cations are monovalent than when they are divalent. Therefore, when the cluster is stressed, more interactions need to be overcome to remove ions from the cluster of a monovalent-neutralized ionomer, leading to higher Young's moduli.

The idea that the local ionic environment is the dominant feature in determining ionomer tensile properties is further supported by two points. First, the ordering of cation types in tensile properties is apparently independent of ionic group concentration. The Young's moduli of the M1C ionomers decrease in the order $Na^+ > Ni^{2+} > Cd^{2+}$, as do the Young's moduli of the M2C ionomers. Polyol type also appears not to affect the trends seen with the different cations. Both sulphonated PTMO(1000)-based and PPO(1000)-based ionomers have Young's moduli decreasing in the order $Na^+ > Cd^{2+} > Ni^{2+}$.

Differential scanning calorimetry

Differential scanning calorimetry (d.s.c.) results for the polyurethane ionomers are summarized in *Table 2*. All ionomers examined except M2CNa exhibited only a well defined glass transition. M2CNa also showed a crystallization exotherm and a melting endotherm. The presence of a detectable degree of crystallinity in M2CNa probably results from the low ion content (59% substitution) of this ionomer, as has been discussed elsewhere[14].

The glass transition temperatures (T_g) of the ionomers are nearly independent of neutralizing cation type. Instead, the glass transition temperatures are determined

Table 1 Tensile properties of model polyurethane ionomers

Sample	Per cent substitution[a]	E_0[b] (MPa)	σ_b (MPa)	ε_b (%)
M1SNa	93	53.7	32.0	710
M1SNi	93	26.0	27.9	340
M1SCd	93	38.8	19.2	600
M1CNa	98	55.7	5.4	310
M1CNi	98	13.8	8.8	420
M1CCd	98	6.6	4.9	700
M2SNa	94	13.5	25.3	740
M2SCd	94	8.2	24.0	760
M2SSr	94	10.5	22.7	750
M2CNa	59	5.6	26.7	1160
M2CNi	59	3.5	24.5	1100
M2CCd	59	2.5	8.0	1200
M2CCa	59	2.4	4.4	1140
P1SNa	95	24.0	0.5	430
P1SNi	95	11.1	2.0	680
P1SCd[c]	95	22.8	–	–
P1SSr	95	36.6	1.8	960
P1SCa	95	47.4	6.7	570

[a] From elemental analysis of the sodium-neutralized ionomers[14]
[b] Zero-strain Young's modulus
[c] Material did not break within the elongation limits of the instrument

Table 2 Differential scanning calorimetry results for model polyurethane ionomers

Sample	Glass transition temperature, T_g (°C)	Crystallization peak (°C)	Crystalline melting peak (°C)
M1SNa	−76	–	–
M1SCa	−75	–	–
M1SMn	−74	–	–
M1SCd	−77	–	–
M1CNa	−67	–	–
M1CNi	−65	–	–
M1CCd	−66	–	–
M2SNa	−80	–	–
M2SNi	−79	–	–
M2SSr	−81	–	–
M2SCd	−80	–	–
M2CNa	−79	−36	14
M2CNi	−79	–	–
M2CCd	−79	–	–
P1SNa	−52	–	–
P1SNi	−47	–	–
P1SCd	−46	–	–
P1SSr	−49	–	–
P1SCa	−48	–	–
P2SNa	−62	–	–
P2SNi	−57	–	–
P2SCd	−60	–	–
P2SSr	−61	–	–
P2SCa	−59	–	–

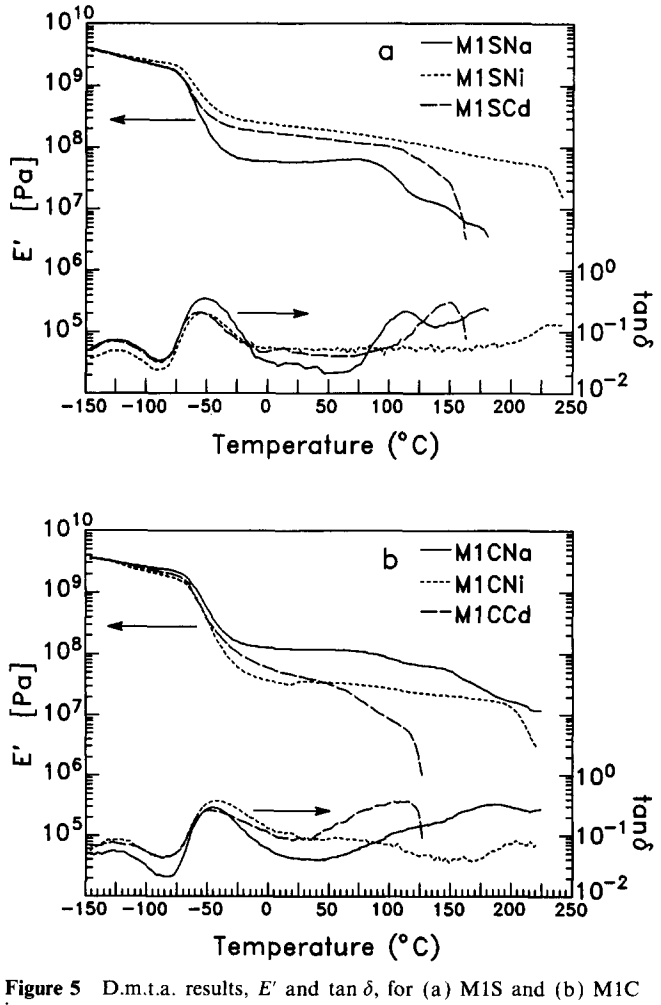

Figure 5 D.m.t.a. results, E' and tan δ, for (a) M1S and (b) M1C ionomers

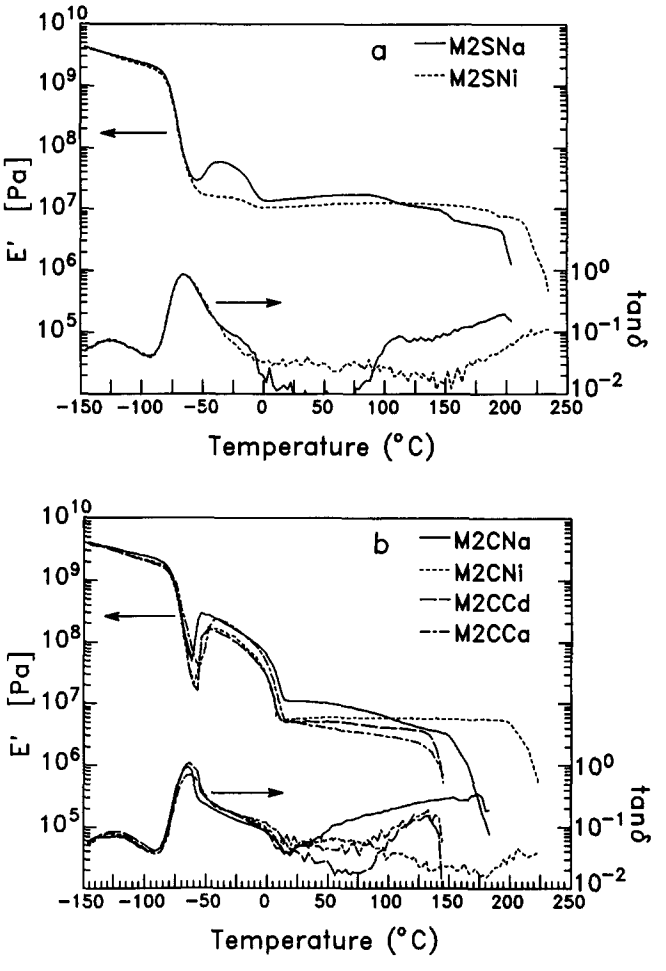

Figure 6 D.m.t.a. results, E' and tan δ, for (a) M2S and (b) M2C ionomers

by polyol type, polyol molecular weight (ionic group content) and pendant anion type. These effects have been discussed in detail elsewhere for the model polyurethane ionomers[14]. As the T_g is primarily determined by the glass transition temperature of the ionomer soft segment (polyol) and the purity of the soft-segment matrix phase, the independence of the T_g from cation type is not surprising. It does, however, indicate similar degrees of phase separation in identical ionomers neutralized with different cations.

Dynamic mechanical thermal analysis

While stress–strain testing provides information about the large-deformation behaviour of ionomers, dynamic mechanical thermal analysis (d.m.t.a.) provides complementary information on the small-deformation behaviour. It also provides information on the thermal characteristics of the ionomers. The storage moduli (E') and loss tangents (tan δ) of the polyurethane ionomers are plotted as a function of temperature in *Figures 5–8*, and the d.m.t.a. results are summarized in *Table 3*. The glass transition temperatures are taken as the maxima in the loss moduli (data not shown). As the scan rates of the d.s.c. (20°C min^{-1}) and the d.m.t.a. (15.9 Hz) experiments are not of comparable time-scales[30], the glass transition temperatures derived from the d.m.t.a. analysis do not agree quantitatively with the T_g values obtained from d.s.c. However, the trends in glass transition temperatures remain the same. T_g is independent of neutralizing cation type but strongly influenced by

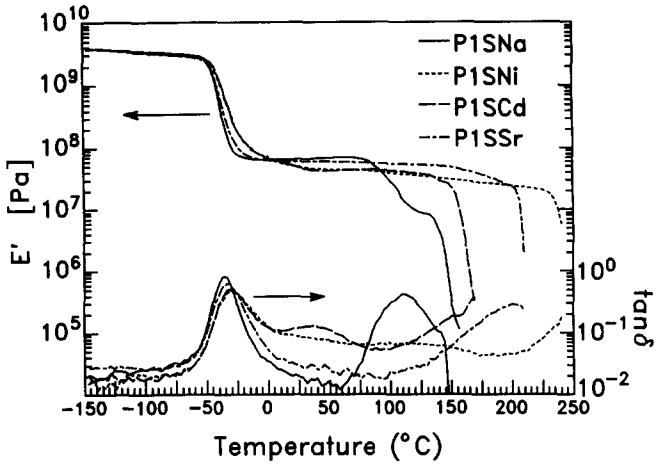

Figure 7 D.m.t.a. results, E' and tan δ, for P1S ionomers

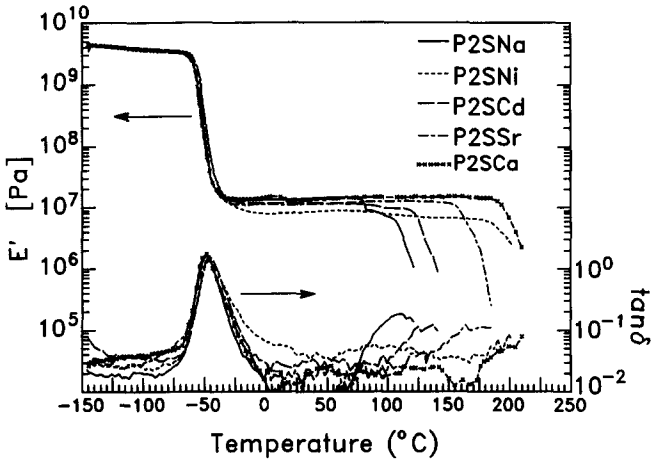

Figure 8 D.m.t.a. results, E' and tan δ, for P2S ionomers

pendant anion type, polyol type and polyol molecular weight, as noted for sodium-neutralized model polyurethane ionomers studied previously[14].

The general features of the E' *versus* temperature curves are characteristic of many ionomer systems[6,11,13]. The well defined glass transition region is followed by an extended rubbery plateau, resulting from ionic aggregation. The presence of crystallinity in the PTMO(2000)-based ionomers is indicated by the broad peak in the E' curves centred at about −45°C. The final downturn in the E' *versus* temperature curves signals the onset of flow in the ionomers, arising from failure of the ionic aggregates as physical crosslinks. The temperature at which the onset of flow occurs is indicative of the strength of the physical crosslinks in these systems. This temperature is consistently highest for the Ni^{2+}-neutralized ionomers and decreases in the order $Ni^{2+} > Na^{+} > Cd^{2+}$ for the PTMO-based ionomers, regardless of pendant anion type. This ordering corresponds well to the trends in Young's moduli observed in the PTMO-based ionomers. The correspondence can be understood by an ion-hopping mechanism[31–33], which postulates that material can flow by redistribution of ionic groups between aggregates without requiring aggregate dissociation. This mechanism and the flow data indicate that ion hopping is most difficult in the Ni^{2+} ionomers and becomes progressively easier in the Na^{+} and Cd^{2+} ionomers. A greater ease of ion hopping allows relaxation of the polyol chains upon the application of stress, causing the Young's moduli to be lower in materials where ion hopping occurs most readily. Thus, a decrease of Young's moduli in the order $Ni^{2+} > Na^{+} > Cd^{2+}$ should be, and is, reflected in a similar ordering of flow temperatures in the d.m.t.a. data.

The glass–rubber inflection point in the E' *versus* temperature curves can be used to characterize the

Table 3 Dynamic mechanical analysis results for polyurethane ionomers

Sample	T_g (°C)	Onset of flow (°C)	T_{in} (°C)	E'_{in} (MPa)	M_e(exp) (g mol^{-1})	$\frac{M_e(\text{calc})}{M_e(\text{exp})}$
M1SNa	−66	189	−37.7	91.2	63.3	15.6
M1SNi	−66	228	−38.8	300	19.1	52.4
M1SCd	−66	132	−45.6	226	24.7	40.5
M1CNa	−58	–	−29.2	170	35.1	28.2
M1CNi	−57	198	−25.4	40.3	150	6.7
M1CCd	−60	108	−25.0	77.1	78.1	12.8
M2SNa	−75	197	−55.3	12.0	444	4.5
M2SNi	−78	209	−55.6	9.8	543	3.7
M2CNa	−75	144	−58.2	11.4	461	4.3
M2CNi	−74	196	−56.8	6.0	886	2.3
M2CCd	−75	135	−57.2	6.3	834	2.4
M2CCa	−74	131	−50.0	8.1	678	2.9
P1SNa	−43	140	−25.4	61.3	111	9.0
P1SNi	−40	232	−14.1	59.3	120	8.3
P1SCd	−40	147	−15.0	50.2	141	7.1
P1SSr	−42	205	−22.4	64.3	107	9.3
P2SNa	−57	103	−40.8	18.0	354	5.7
P2SNi	−54	177	−38.1	8.6	750	2.6
P2SCd	−53	122	−38.8	12.0	536	3.7
P2SSr	−57	154	−41.5	9.8	649	3.1
P2SCa	−57	191	−43.8	12.4	508	3.9

thermal and mechanical properties of the ionomers as well. Density (ρ) values of 0.98 g cm^{-3} for PTMO[34] and 1.1 g cm^{-3} for PPO[35] can be combined with the values of the storage modulus (E'_{in}) and temperature (T_{in}) at the glass–rubber inflection point to calculate the average molecular weight between crosslinks according to the equation[36]:

$$M_c(\text{exp}) = 3\rho RT_{in}/E'_{in}$$

These values are reported in *Table 3*. The crosslinking efficiency of the ionic aggregates may be expressed as the ratio $M_c(\text{calc})/M_c(\text{exp})$, where $M_c(\text{calc})$ is the theoretical value for strictly multiplet-type[37] interactions and is taken as the molecular weight of the polyol segments. This method allows comparison of the state of ionic aggregation in the ionomers with respect to a reference state, in this case a state where only multiplet-type interactions occur ($M_c(\text{calc})$). Larger values of $M_c(\text{calc})/M_c(\text{exp})$ indicate enhanced states of ionic aggregation. It should be noted that strict application of this equation makes assumptions regarding ionomer morphology that may not be strictly correct. While the trends displayed should remain valid regardless of the inherent differences between chemically crosslinked polymers and ionomers, caution should be exercised in using the absolute values of M_c calculated here as bases for comparison with other polymer systems.

As has been seen for other thermal and mechanical properties of the polyurethane ionomers, the $M_c(\text{calc})/M_c(\text{exp})$ ratio is strongly influenced by pendant anion and neutralizing cation type[14]. The ratio decreases in the order $Na^+ > Cd^{2+} > Ni^{2+}$ for the carboxylated PTMO(1000)-based ionomers. Small-angle X-ray scattering (SAXS) data presented in the next section for the carboxylated ionomers indicate that the $M_c(\text{calc})/M_c(\text{exp})$ ratio, a measure of crosslinking efficiency, is directly correlated to the number of ionic groups in the ionic aggregates (n). As the calculated n values should reflect the crosslink functionalities of the ionomers, it is seen that the basic tenets of rubber elasticity theory appear to hold in this system as well. Higher crosslink functionalities result in higher $M_c(\text{calc})/M_c(\text{exp})$ values, which correspond to higher inflection modulus values. Thus, low-temperature modulus values are directly related to the functionality of the physical crosslinks, as would be intuitively predicted.

The trend in the $M_c(\text{calc})/M_c(\text{exp})$ ratio for the carboxylated PTMO(2000)-based ionomers matches that of the M1C ionomers; in the M2C ionomers, the ratio decreases in the order $Na^+ > Ca^{2+} > Cd^{2+} > Ni^{2+}$. The trend is again mirrored by the n values derived from SAXS (see *Table 5*) for M2CNa and M2CNi.

The sulphonated PTMO(1000)-based ionomers display a slightly different ordering in $M_c(\text{calc})/M_c(\text{exp})$ values; the ratio decreases in the order $Ni^{2+} > Cd^{2+} > Na^+$. It can be postulated that crosslink functionality is an important factor in these systems. The crosslink functionality will be partially determined by the geometric packing constraints of the ionic groups. Thus, just as the planar nature of the carboxylate anion is postulated to have different coordination tendencies with certain cations than the tetrahedral sulphonate anion, so it could also give rise to different crosslink functionalities with certain cation types. Such an idea is supported by the different n values obtained from SAXS analysis, detailed below, of M1SNa ($n = 124$) and M1CNa ($n = 244$).

In addition to pendant anion type, polyol type also influences the $M_c(\text{calc})/M_c(\text{exp})$ ratios. The ratios, or crosslinking efficiencies, are much lower for the P1S ionomers than for the PTMO(1000)-based ionomers. As discussed elsewhere[38], the larger chain cross-section of the PPO-based ionomers could prevent aggregation of large numbers of ionic groups into single clusters. Thus, crosslink functionalities would necessarily be lower, as would crosslinking efficiencies. The different trends in crosslinking efficiencies for the various cation types could also result from the dissimilar characteristics of the backbone types. The trend in $M_c(\text{calc})/M_c(\text{exp})$ ratios for the P1S ionomers is $Sr^{2+} > Na^+ > Ni^{2+} > Cd^{2+}$, in contrast to the order $Ni^{2+} > Cd^{2+} > Na^+$ for the M1S ionomers. Once again, however, the trend in crosslinking efficiencies is matched by the trends in the number of ionic groups per aggregate, n, as discussed below. Apparently, the influences of backbone and cation cannot be completely deconvoluted in polyurethane ionomers.

The influences of polyol molecular weight, or ionic group content, and cation type are also difficult to separate. The $M_c(\text{calc})/M_c(\text{exp})$ ratio for P2S ionomers decreases in the order $Na^+ > Ca^{2+} > Cd^{2+} > Sr^{2+} > Ni^{2+}$, unlike its PPO(1000)-based analogue. Differences here may be understood by considering variations in ionic packing arrangements. Analysis of P1SNa and P2SNa indicated large differences in the overall degree of order in the ionomer morphologies[38]; SAXS results for P1SNa displayed four scattering peaks whose spacings corresponded to a simple cubic or body-centred cubic lattice arrangement for the ionic aggregates. No evidence of such a highly ordered structure was seen for P2SNa. In addition, local packing densities in the ionic aggregates were postulated to be different for P1SNa and P2SNa on the basis of the SAXS analysis; the cations were more densely packed in the ionic aggregates of P1SNa. Given the overall microstructural mismatch and the local aggregate packing differences in P1SNa and P2SNa, as well as the above discussion of the role of local packing considerations in determining ionomer properties, it is not surprising that different cation $M_c(\text{calc})/M_c(\text{exp})$ orderings are seen for the sulphonated PPO(1000)- and PPO(2000)-based ionomers.

Small-angle X-ray scattering

The small-angle X-ray scattering (SAXS) patterns for some of the model polyurethane ionomers are shown in *Figures 9–11*. The scattering patterns show the two features typical of ionomer SAXS data: an upturn at low scattering vector q, which has been attributed to an inhomogeneous distribution of ionic groups[39,40], and a peak or shoulder on the upturn, which is indicative of ionic aggregation and is usually referred to as the 'ionomer peak.'

In order to analyse the data, they were fitted to a modified liquid-like interparticle interference model, which attributes the ionomer peak to interparticle scattering. The model, originally proposed by Yarusso and Cooper[10], has been modified to include the Percus–Yevick[41] total correlation function, as solved by Wertheim[42] and Thiele[43], instead of the Fournet three-body interaction function originally utilized. An evaluation of the modified model has confirmed its usefulness in modelling polyurethane ionomer SAXS data[38]. The model has four fitting parameters: R_1, the radius of the spherical ionic aggregate cores; R_2 ($R_2 > R_1$), the radius

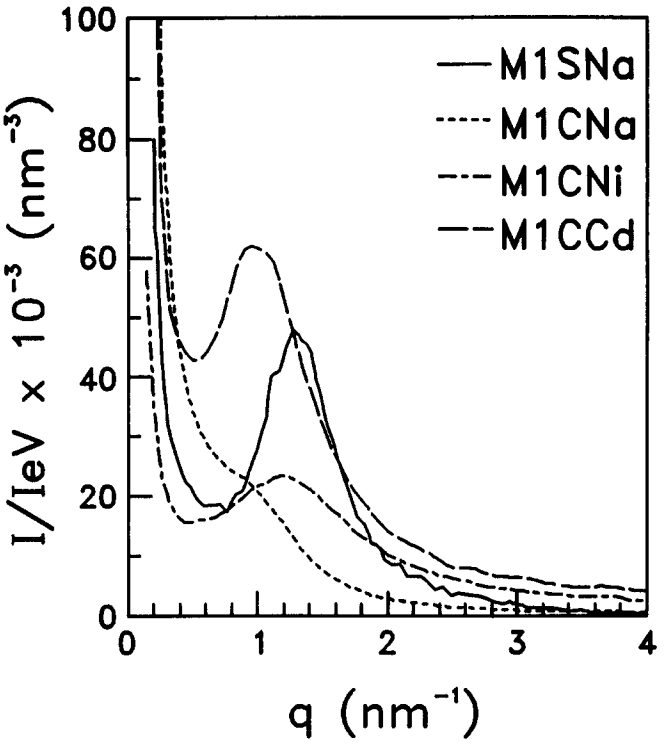

Figure 9 Small-angle X-ray scattering patterns for PTMO(1000)-based ionomers

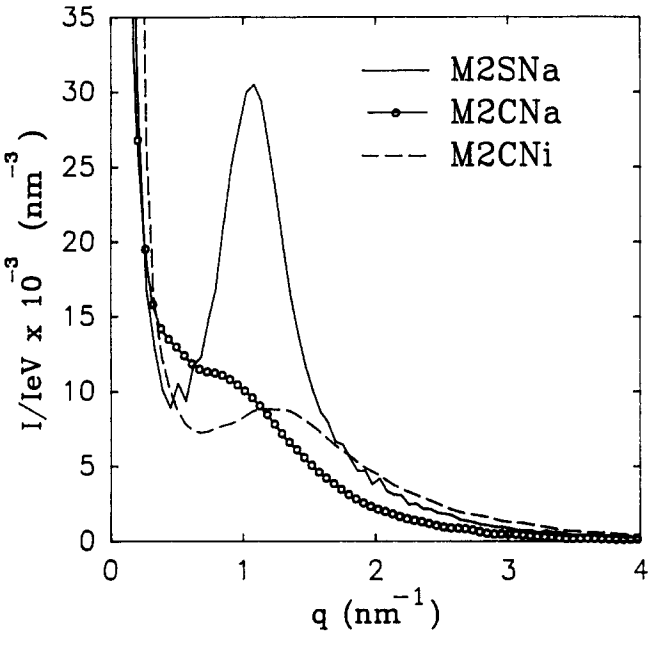

Figure 10 Small-angle X-ray scattering patterns for PTMO(2000)-based ionomers

of the polymer sheath surrounding the ionic cores (the sheath arises from the connectivity of the ionic groups and the polymer backbone); v_p, the volume of material per ionic aggregate (the inverse of the aggregate number density); and $\Delta\rho$, the electron density difference between the aggregates and the matrix. The model fitting results for the polyurethane ionomers examined by SAXS are given in *Table 4*.

Since an interparticle interference model is postulated, the q value at which the maximum in intensity is attained, q^*, is inversely related to interaggregate spacings. For the M1C ionomers, q^* increases in the order $Ni^{2+} > Cd^{2+} > Na^+$, implying an inverse trend in average spacing between the aggregates. A similar trend of q^* values is seen for the M2C ionomers, with q^* decreasing from Ni^{2+} to Na^+. In the P1S ionomers, q^* increases in the order $Ni^{2+} < Na^+ < Sr^{2+} < Ca^{2+} < Cd^{2+}$. This implies that the average spacing between the aggregates decreases in the same order, with Ni^{2+} giving the largest average interaggregate spacing and Cd^{2+} the smallest. This trend is exactly reflected in the v_p values. The similarity of the q^* values for the P1S ionomers neutralized with different cations, as well as the similarity of their v_p values, indicates that the P1S ionomers possess

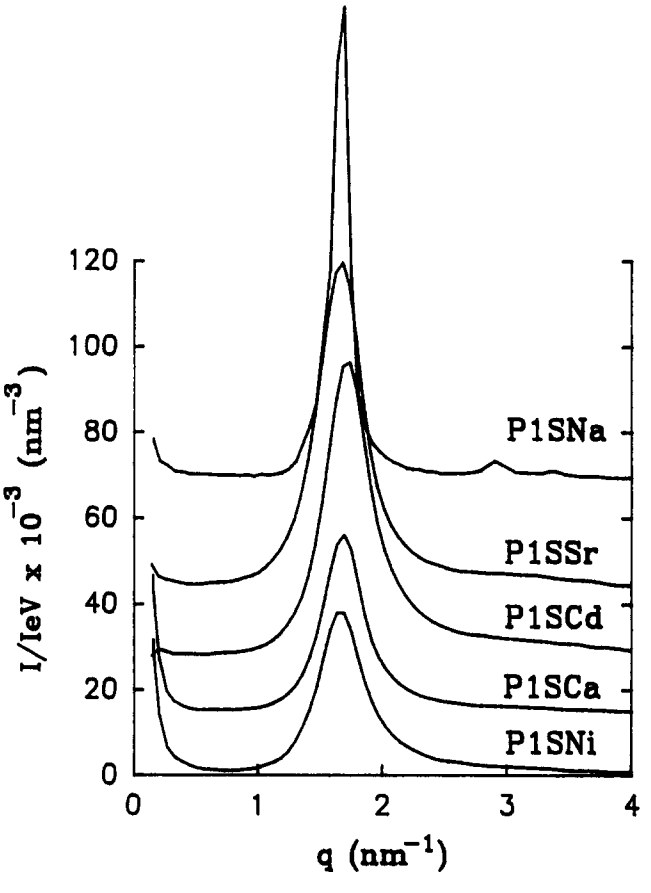

Figure 11 Small-angle X-ray scattering patterns for P1S ionomers. Curves are arbitrarily offset for clarity

Table 4 Small-angle X-ray scattering model parameters

Sample	R_1 (nm)	R_2 (nm)	v_p (nm^3)	$\Delta\rho$ (nm^{-3})	g^a
M1SNa	1.46	2.30	278	264	0.073
M1CNa	1.70	2.94	842	261	0.024
M1CNi	1.18	2.16	301	442	0.023
M1CCd	1.47	2.67	500	481	0.028
M2SNa	1.59	2.76	332	222	0.012
M2CNa	1.47	2.76	1362	342	0.010
M2CNi	1.06	2.04	317	391	0.016
P1SNa	1.11	2.21	77	319	0.074
P1SNi	1.14	2.00	77	273	0.081
P1SCa	1.20	2.01	75	241	0.097
P1SSr	1.23	2.00	76	322	0.103
P1SCd	1.03	1.96	71	454	0.065

[a] $g = 4\pi R_1^3/3v_p$, the volume fraction of ionic aggregates

Table 5 Crystalline model compounds and calculated numbers of ionic groups in aggregates

Ionomer	Model compound	Ref.	n
M1SNa	CH_3NaO_3S	45	124
M1CNa	$NaH(C_2H_3O_2)_2$	46	244
M1CNi	$Ni(CH_3CO_2)\cdot 4H_2O$	47	59
M1CCd	$Cd(CH_3CO_2)_2\cdot 2H_2O$	48	127
M2SNa	CH_3NaO_3S	45	160
M2CNa	$NaH(C_2H_3O_2)_2$	46	158
M2CNi	$Ni(CH_3CO_2)\cdot 4H_2O$	47	43
P1SNa	CH_3NaO_3S	45	54
P1SNi	$NiS_2O_6\cdot 6H_2O$	49	46
P1SCa	$Ca(SO_3CH_2SO_3)\cdot 3H_2O$	50	67
P1SSr	$SrSO_4$	51	87
P1SCd	$Cd(SO_3CH_2SO_3)\cdot 3H_2O$	50	42

similar degrees of phase separation regardless of cation type. It also implies that the differences in physical properties for these ionomers are attributable to the cation chemistry, as suggested above. The regular morphology of the P1S ionomers is indicated by the narrowness of their first-order scattering peaks. The regular placement of the ionic aggregates is also deduced from the modelling parameters; the distances of closest approach $2R_2$ are approximately equal to $v_p^{1/3}$ for all the sulphonated PPO(1000)-based ionomers.

Morphological differences based on cation type can be observed directly in the scattering patterns for the P1S ionomers shown in *Figure 11*. (The SAXS curves for the P1S ionomers have been arbitrarily offset for clarity.) While none of the ionomers neutralized with divalent cations displayed higher-order scattering peaks, P1SNa displayed three higher-order peaks. Another paper presents an analysis of the implications of the higher-order scattering peaks on the morphology of P1SNa[38]. The use of narrow molecular-weight distribution ionomer chains in SAXS studies of NaSPS ionomers permitted observation of fine structure on the ionomer peak[21]; perhaps the regular architecture of the P1SNa ionomer similarly allowed the unusual properties of the Na^+ cation to manifest themselves, resulting in a more ordered morphology.

The volume fraction of ionic aggregates, g, is seen to be relatively low, less than about 10%, for the polyurethane ionomers, as would be expected based on the chemistry of these systems. While the g values seem to be dependent on anion type and polyol molecular weight, they are fairly independent of cation type and polyol type. The similarity of g values for M1SNa and the sulphonated PPO(1000)-based ionomers indicates similar degrees of phase separation in these materials, suggesting that pendant anion type is predominantly responsible for determining the phase mixedness of ionomers. The relative independence of the g values from cation type and polyol type suggests the important role the pendant anion plays in determining ionomer phase morphology.

Unlike the ionic aggregate volume fraction, the size of the ionic aggregates is dependent on cation type. For the PTMO-based ionomers, the ionomers neutralized with the monovalent sodium cation have consistently larger ionic core radii (R_1) than the ionomers neutralized with divalent cations. If the local packing constraints of the monovalent and divalent cations are considered, Lefelar and Weiss[29] have argued that there are more orientations of anion and cation available for adding additional ionic groups to an aggregate if the cation is monovalent. Thus, entropy considerations favour aggregate enlargement more for monovalent than divalent cations. A similar argument rationalizes the trend of decreasing R_1 values with increasing cation valency seen earlier for lower-molecular-weight sulphonated PTMO-(1000)-based ionomers[44].

Using crystallographic data from low-molecular-weight model compounds, the R_1 values are utilized to compute the number of ionic groups per aggregate n by:

$$n = \frac{Z}{V}\left(\frac{4\pi R_1^3}{3}\right)$$

where Z is the number of ionic groups in the unit cell of the model compound and V is the volume of the unit cell. Crystallographic data from the model compounds listed in *Table 5* were used. Note that model compounds were selected to be consistent within an anion type; thus, metal acetates and metal methanesulphonates were selected, when crystallographic data were available. It is not suggested that the crystallographic structure of the model compounds exactly matches the aggregate packing arrangements in the ionomers, and the n values calculated here are used solely for comparison of trends for ionomers of similar anion type. Differences in the crystallographic structures of the model compounds arise primarily from the influence of the particular cation, as is the case for the model polyurethane ionomers, making the model compounds useful bases for comparison.

The calculated n values appear in *Table 5*. While it cannot be said that the n values attained from these calculations are quantitatively correct, these calculations do allow comparison of values that take into account the particular chemistry of each cation. It is noteworthy that the arguments for a greater number of ionic groups in the ionic aggregates of ionomers neutralized with monovalent than divalent cations still holds when n values are compared. Thus, the method is internally consistent. The n values may be regarded as a measure of the functionality of the physical crosslinks in these ionomers and thus correlated to the physical property trends. Just as the crosslinking efficiency determined from the d.m.t.a. data increased in the order $Ni^{2+} < Cd^{2+} < Na^+$, so also do the n values for the M1C ionomers. The correlation of n values and $M_c(\text{calc})/M_c(\text{exp})$ ratios also holds for a different polyol type and a different pendant anion type. For the P1S ionomers, $M_c(\text{calc})/M_c(\text{exp})$ and n both increase in the order $Cd^{2+} < Ni^{2+} < Na^+ < Ca^{2+} < Sr^{2+}$. Thus, these limited data imply that cation type strongly influences crosslink functionality, which in turn determines the inflection moduli of the polyurethane ionomers.

CONCLUSIONS

The influence of cation type on the morphology and properties of model polyurethane ionomers has been studied in ionomers with different backbone types, pendant anion types and ionic group concentrations. A strong correlation between the degree of ordering in the immediate vicinity of the neutralizing cation[27] and the large-deformation properties of the ionomers was observed. An ion-hopping mechanism can rationalize this result. As the local environment of the cation becomes more ordered, enthalpic constraints produce a higher

energy barrier for removal of ionic groups from the aggregates. Since aggregate rearrangement is hindered when ion hopping is difficult, the physical crosslinks behave more like permanent chemical crosslinks, imparting strength and stiffness to the ionomer. In ionomers neutralized with cations that induce a high degree of local ordering, ion hopping is difficult, and the resulting ionomer is stiff.

The importance of geometrical constraints of the ionic groups was also observed for the different pendant anion types. The planar carboxylate anion was postulated to complex with the neutralizing cation in a different manner than the tetrahedral sulphonate anion, producing different trends in mechanical properties with varying cation types. The differences seen here suggest that there is no 'universal ordering' of cations that can be used to predict ionomer properties *a priori*. However, consideration of the electronic and geometrical properties of the anion and cation can give a sound indication of trends in physical properties.

This idea was particularly emphasized by the SAXS analysis of the ionomers. Calculations of the number of ionic groups per aggregate were performed using model compounds of matching anion and cation type. Direct correspondences as cation type was varied between the small-strain modulus values at low temperatures and the number of ionic groups per aggregate were observed. The data allow it to be argued that cation and anion type govern the local packing arrangements of the cations. The local environment determines the aggregate morphology, and the aggregate structure influences the overall morphology and properties of the ionomers. Thus, the results in this paper suggest that the local packing of the ionic aggregates is a more important factor in determining ionomer properties than previously realized.

ACKNOWLEDGEMENTS

Support for this work was provided by US Department of Energy through Grant DE-FG02-88ER45370; by the donors of the Petroleum Research Fund, administered by the American Chemical Society, through Grant 20343-AC7; and by Fellowships for S.A.V. from the National Science Foundation and the Wisconsin Alumni Research Foundation. Special thanks are due to Wade Wolfe and Richard Reiner for their help in collecting some of the tensile testing and d.m.t.a. data presented in this work.

REFERENCES

1 Eisenberg, A. and King, M. 'Ion Containing Polymers: Physical Properties and Structure', Academic Press, New York, 1977
2 MacKnight, W. J. and Earnest, T. *Macromol. Sci., Rev. Macromol. Chem.* 1981, **16**, 41
3 Eisenberg, A. and Bailey, F. (Eds.) 'Coulombic Interactions in Macromolecular Systems', ACS Symp. Ser. 302, American Chemical Society, Washington, DC, 1986
4 Tant, M. and Wilkes, G. *J. Macromol. Sci., Rev. (C)* 1988, **28**, 1
5 Lantman, C. W., MacKnight, W. J. and Lundberg, R. D. *Annu. Rev. Mater. Sci.* 1989, **19**, 295
6 Fitzgerald, J. J. and Weiss, R. A. *J. Macromol. Sci., Rev. (C)* 1988, **28**, 99
7 Lundberg, R. D. in 'Structure and Properties of Ionomers', (Eds. M. Pineri and A. Eisenberg), Reidel, Boston, 1987, p. 429
8 Weiss, R. A., MacKnight, W. J., Lundberg, R. D., Mauritz, K. A., Thies, C. and Brant, D. A. in 'Coulombic Interactions in Macromolecular Systems', (Eds. A. Eisenberg and F. Bailey), ACS Symp. Ser 302, American Chemical Society, Washington, DC, 1986
9 Brockman, N. L. and Eisenberg, A. *J. Polym. Sci., Polym. Phys. Edn.* 1985, **23**, 1145
10 Yarusso, D. J. and Cooper, S. L. *Macromolecules* 1983, **16**, 1871
11 Gauthier, M. and Eisenberg, A. *Macromolecules* 1989, **22**, 3754
12 Gauthier, M. and Eisenberg, A. *Macromolecules* 1990, **23**, 2066
13 Ding, Y. S., Register, R. A., Yang, C.-Z. and Cooper, S. L. *Polymer* 1989, **30**, 1204
14 Visser, S. A. and Cooper, S. L. *Macromolecules* 1991, **24**, 2576
15 Hashimoto, T., Fujimura, M. and Kawai, H. in 'Perfluorinated Ionomer Membranes', (Eds. A. Eisenberg and H. L. Yeager), ACS Symp. Ser. 180, American Chemical Society, Washington, DC, 1982, p. 217
16 Lundberg, R. D. and Makowski, H. S. in 'Ions in Polymers', (Ed. A. Eisenberg), ACS Symp. Ser. 187, American Chemical Society, Washington, DC, 1986
17 Register, R. A., Foucart, M., Jerome, R., Ding, Y. S. and Cooper, S. L. *Macromolecules* 1988, **21**, 1009
18 Broze, B., Jerome, R., Teyssie, Ph. and Marco, C. *Macromolecules* 1983, **16**, 996
19 Yarusso, D. J., Ding, Y. S., Pan, H. K. and Cooper, S. L. *J. Polym. Sci., Polym. Phys. Edn.* 1984, **22**, 2073
20 Yarusso, D. J. and Cooper, S. L. *Polymer* 1985, **26**, 371
21 Chu, B., Wu, D.-Q., MacKnight, W. J., Wu, C., Phillips, J. C., LeGrand, A., Lantman, C. W. and Lundberg, R. D. *Macromolecules* 1988, **21**, 523
22 Eisenberg, A., Hird, B. and Moore, R. B. *Macromolecules* 1990, **23**, 4098
23 Lake, J. A. *Acta Crystallogr.* 1967, **23**, 191
24 Kratky, O., Pilz, I. and Schmitz, P. J. *J. Colloid Interface Sci.* 1966, **21**, 24
25 Porod, G. *Kolloid Z.* 1951, **124**, 83
26 Ding, Y. S., Register, R. A., Yang, C.-Z. and Cooper, S. L. *Polymer* 1989, **30**, 1221
27 Visser, S. A. and Cooper, S. L. *Polymer* 1992, **33**, 930
28 Wells, A. F. 'Structural Inorganic Chemistry', 5th Edn., Oxford University Press, New York, 1984
29 Lefelar, J. A. and Weiss, R. A. *Macromolecules* 1984, **17**, 1145
30 Sperling, L. H. 'Introduction to Physical Polymer Science', Wiley, New York, 1986
31 Ward, T. C. and Tobolsky, A. V. *J. Appl. Polym. Sci.* 1967, **11**, 2903
32 Sakamoto, K., MacKnight, W. J. and Porter, R. S. *J. Polym. Sci. (A-2)* 1970, **8**, 277
33 Hara, M., Eisenberg, A., Storey, R. F. and Kennedy, J. P. in 'Coulombic Interactions in Macromolecular Systems', (Eds. A. Eisenberg and F. Bailey), ACS Symp. Ser. 302, American Chemical Society, Washington, DC, 1986, p. 302
34 Vallance, M. A. and Cooper, S. L. *Macromolecules* 1984, **17**, 1208
35 Clough, S. B. and Schneider, N. *J. Macromol. Sci., Phys.* 1968, **2**, 553
36 Treloar, L. R. G. 'The Physics of Rubber Elasticity', Oxford University Press, Oxford, 1958, Ch. 9
37 Eisenberg, A. *Macromolecules* 1970, **3**, 147
38 Visser, S. A. and Cooper, S. L. *Macromolecules* 1991, **24**, 2584
39 Register, R. A., Pruckmayr, G. and Cooper, S. L. *Macromolecules* 1990, **23**, 3023
40 Register, R. A., Cooper, S. L., Thiyagarajan, P., Chakrapani, S. and Jerome, R. *Macromolecules* 1990, **23**, 2978
41 Percus, J. K. and Yevick, G. *Phys. Rev.* 1958, **110**, 1
42 Wertheim, J. S. *Phys. Rev. Lett.* 1963, **10**, 321
43 Thiele, E. *J. Chem. Phys.* 1963, **39**, 474
44 Ding, Y. S., Register, R. A., Yang, C.-Z. and Cooper, S. L. *Polymer* 1989, **30**, 1213
45 Ferguson, G. and Scrimgeour, S. N. (Eds.) 'Structure Reports for 1981', Vol. 48B, Reidel, Boston, 1986, p. 66
46 Wyckoff, R. W. G. 'Crystal Structures', 2nd Edn., Vol. 5, Interscience, New York, 1966, p. 324
47 Trotter, J. (Ed.) 'Structure Reports for 1971', Vol. 37B, Oosthock, Scheltema and Holkema, Utrecht, 1975, p. 506
48 Trotter, J. and Ferguson, G. (Eds.) 'Structure Reports for 1972', Vol. 38B, Oosthock, Scheltema and Holkema, Utrecht, 1975, p. 874
49 Wyckoff, R. W. G. 'Crystal Structures', 2nd Edn., Vol. 5, Interscience, New York, 1966, p. 554
50 Ferguson, G. and Iball, J. (Eds.) 'Structure Reports for 1979', Vol. 45B, Reidel, Boston, 1984, p. 49
51 Wyckoff, R. W. G. 'Crystal Structures', 2nd Edn., Vol. 5, Interscience, New York, 1966, p. 56